

Quantum-Secure Authentication with a Classical Key

Sebastianus A. Goorden¹, Marcel Horstmann^{1,2}, Allard P. Mosk¹, Boris Škorić³, and Pepijn W.H. Pinkse^{1,4}

Authentication provides the trust people need to engage in transactions. The advent of physical keys that are impossible to copy promises to revolutionize this field. Up to now, such keys have been verified by classical challenge-response protocols [1, 2, 3, 4, 5, 6, 7, 8]. Such keys are in general susceptible to emulation attacks. Here we demonstrate Quantum-Secure Authentication (“QSA”) of an unclonable classical physical key in a way that is inherently secure by virtue of quantum-physical principles [9, 10, 11, 12]. Our quantum-secure authentication operates in the limit of a large number of channels, represented by the more than thousand degrees of freedom of an optical wavefront shaped with a spatial light modulator [13]. This allows us to reach quantum security with weak coherent pulses of light containing dozens of photons, too few for an adversary to determine their complex spatial shapes, thereby rigorously preventing emulation.

A Physical Unclonable Function (PUF) is a key that cannot be copied because its manufacture inherently contains uncontrollable steps [1, 3]. Such a physical key is a function in the sense that it reacts to a stimulus (“challenge”) with a response. After manufacture there is a one-time characterization of the key in which its challenge-response behavior is stored in a database. The key can then be authenticated by comparing its response behavior to the database. An excellent optical implementation of an unclonable key is provided by a medium containing a high density of scatterers at random positions, supporting many independent challenge-response pairs [1, 14, 15]. As challenges for such a key we use laser pulses, each with a carefully shaped wavefront. The corresponding responses are the reflected wavefronts, which are speckle patterns and depend strongly on the challenges as well as on the positions of the scatterers. Authentication consists of sending challenges to the key and comparing the obtained responses to the responses found in the database, as illustrated in Fig. 1a. Only if the responses match, the key is accepted.

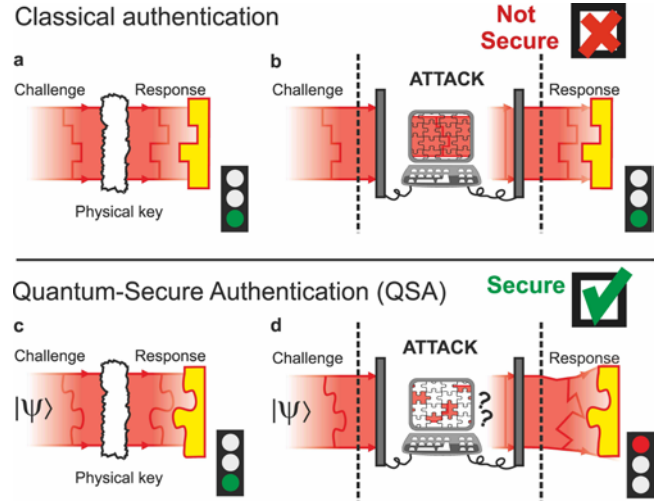


Figure 1| The idea of Quantum-Secure Authentication (QSA): **a**, In classical authentication of an optical unclonable physical key, a challenge wavefront of sufficient complexity is sent to the key. The response wavefront is compared with those stored in a database (yellow pieces) to make a pass (green light) or fail (red light) decision. However, this verification can be spoofed by an emulation attack (**b**) in which the challenge wavefront is completely determined and the expected response is constructed by the adversary who knows the challenge-response behavior of the key. In Quantum-Secure Authentication (**c**) the challenge is a quantum state for which an emulation attack (**d**) fails because the adversary cannot actually determine the quantum state and hence any attempt to generate the correct response wavefront fails.

Although it is impossible to copy or all-optically emulate the key (see Appendix), classical authentication is not unconditionally secure because of the risk of digital emulation (Fig. 1b). An adversary who knows the challenge-response behavior of the key can measure the challenge and can fool the verifier by returning a response that is generated by alternative means, for example with a spatial light modulator (SLM). Emulation attacks can be impeded by requiring the owner of the key to entrust the key to the verifier, human inspection or anti-spoofing sensors. Attackers try to fool the anti-spoofing sensors, leading to an arms race that is expensive and inefficient.

Quantum-Secure Authentication (QSA) provides a solution by basing the security of the readout of the key on quantum-physical principles [16]. Quantum readout of physical keys exploits the non-cloning property of quantum states to hide challenges from the adversary, much in the style of quantum cryptography [9, 10, 17]. Since the challenges are quantum states, the adversary is unable to fully determine the challenges and thus cannot emulate the response states (Fig. 1c-d).

¹ Complex Photonic Systems (COPS), MESA+ Institute for Nanotechnology, University of Twente, PO Box 217, 7500 AE Enschede, The Netherlands

² Laser Physics and Nonlinear Optics, MESA+ Institute for Nanotechnology, University of Twente, PO Box 217, 7500 AE Enschede, The Netherlands

³ Eindhoven University of Technology, PO Box 513, 5600 MB Eindhoven, The Netherlands

⁴ Applied Nanophotonics, MESA+ Institute for Nanotechnology, University of Twente, PO Box 217, 7500 AE Enschede, The Netherlands.

Here we demonstrate Quantum-Secure Authentication of a physical object, exploiting the highly robust coherent states of light with a low mean photon number [18]. In principle, quantum readout of optical PUFs can also be achieved with single or bi-photon states [19], squeezed states [20] or other fragile quantum states [11]. We choose coherent states of light with low mean photon number, because they will be easier to implement in real-life applications. Quantum security is achieved thanks to a specific property of high-spatial-dimension quantum fields [21, 22, 23]: On the one hand, the shape of the spatial wave function contains much more information than can be classically read out because of unavoidable quantum readout noise in a measurement. On the other hand, the presence of the encoded information can be easily verified by an appropriate basis transformation. We exploit this quantum phenomenon by constructing low-photon-number light pulses with wavefronts of high complexity [13] and then efficiently verifying the response wavefronts.

Our key consists of a multiple-scattering layer of pigment nanoparticles. After its manufacture, the key is enrolled: a number of challenge-response pairs is measured with as much light as needed. Each of our challenges is described by a 50×50 binary matrix. Each element corresponds to a phase of either 0 or π . A spatial light modulator (SLM1) is used to transform the incoming plane wavefront into the desired challenge wavefront. The challenge is sent to the key and the reflected field is recorded in a phase-sensitive way. The challenge along with the corresponding response is stored in a challenge-response database.

After enrolment, keys can be authenticated using the setup illustrated in Fig. 2. A challenge-response pair is selected from the database. SLM1 is used to construct the challenge wavefront, which is then sent to the key. The reflected wavefront is sent to SLM2, which adds to it the conjugate phase pattern of the expected response wavefront. Therefore, SLM2 transforms the reflected speckle field into a plane wave only when the response is correct. In case the response is wrong, SLM2 transforms the field into a completely different speckle field. When the response is correct, the lens positioned behind SLM2 focuses the plane wave to a point in the analyzer plane, as shown in Fig. 2b. A false key will result in a low-intensity speckle on the analyzer plane as shown in Fig. 2c. Compared to the typical peak height in Fig. 2b of 1000 times the background, the loss of intensity in the center of Fig. 2c is dramatic. This method therefore allows fast discriminative readout with a single-pixel detector in the center of the image plane.

QSA exploits the bright central peak in the analyser plane for photodetection at the single quantum level. To this end we attenuate our coherent light source and chop it into 500 ns light pulses each containing $n = 230 \pm 40$ photons. Pulses are sufficiently far apart that SLM1 can imprint a different

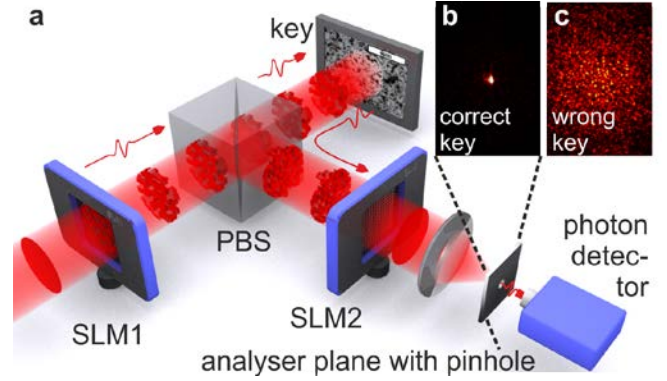


Figure 2| Quantum-secure optical readout of a physical key. **a**, Setup: A spatial light modulator (SLM1) creates the challenge by phase shaping a few-photon wavefront. In the experiment a 50×50 binary phase pattern is used with 0 and π phase delays. The challenge is sent to the key, a ZnO key (scale bar is $4 \mu\text{m}$), by a microscope objective (not shown). The response is coupled out by a polarising beam splitter (PBS). The response is transformed back by SLM2 and then focused onto the analyser plane. **b**, Only if the key was the true unique key, the response has a bright spot in the centre, holding $\approx 60\%$ of the power in the image and allowing that fraction to pass a pinhole and land on a detector where photodetection clicks authenticate the key. **c**, In case of a false key, the response in the analyser plane is a random speckle pattern.

challenge wavefront onto each pulse. After passing the key and SLM2 we spatially filter the field in the analyser plane with a pinhole and image it onto a photon-counting detector. In Fig. 3a we show the typical photodetector signal for the correct response and for an incorrect response provided by the true and a false key, respectively. Only with the true key multiple photodetections are seen. After repeating the measurement 2000 times, Fig. 3b shows the histogram of the number of photodetections for the true key, resembling a Poissonian distribution with a mean of 4.3. Fig. 3b also shows the average histogram of photodetections when 5000 random challenges are sent to the key, with the key and SLM2 kept unchanged. This experiment gives an upper bound on the photodetections in case of an attack with a random key. This histogram resembles a Poissonian distribution with a mean of 0.016 photodetections. We hence see that we can clearly discriminate between true and false keys.

In order to characterize the achievable security for one repetition of our readout, we introduce the quantum security parameter S ,

$$S \equiv K/n \quad (1)$$

as the ratio of the number of controlled modes K and the average number of photons n in the challenge. The

parameter K quantifies the complexity of the challenge wavefront and is identical to the number of independent response wavefronts that are obtained by sending in different challenge wavefronts. It is well approximated by the number of speckles on the key illuminated by the challenge [24]. In our experiment we have $K = 1100 \pm 200$ and $n = 230$, yielding $S = 5 \pm 1$. Because a measurement of a photon can extract only a limited amount of information, a large S implies that the adversary can only obtain a small fraction of the information required to characterize the challenge. Therefore he cannot determine the correct response. An adversary who measures an optimal choice of field quadratures of the challenge cannot achieve better than approximately [25]

$$|\gamma|^2 = |\gamma_{OK}|^2 / (S+1), \quad (2)$$

where $|\gamma|^2$ is the fraction of photons detected by the verifier's hardware in case of an attack and $|\gamma_{OK}|^2$ is the fraction of photons detected when the response is correct. This result holds for $S > 1$ and $K \gg 1$ and is in line with the intuition that a measurement of n photons can only provide information about n modes. Operating the readout in the regime $S > 1$ therefore gives the verifier an eminent security advantage which has its origin in the quantum character of the light. Note that we exclude the possibility that the adversary uses quantum-computational tools, since that would require a K -qubit quantum-computation system with low error rate, which is far beyond the capabilities of foreseeable technology [26].

In the verification we aim to discriminate a correct key from a challenge-estimation attack. Given a conservative lower bound of $S = 4$, the number of photodetections on the single-photon detector in a single readout in case of an optimal attack follows a Poissonian distribution with mean 0.86, as shown in Fig. 3b. Choosing a threshold of 3 or more photodetections for accepting the key, we find that the measured false reject ratio is 9%. In case of random challenges the false accept ratio is 1.7×10^{-4} % and the theoretical maximum false accept probability in case of the challenge-estimation attack (Eq. 2) is 6% (Fig. 3c). The security improves exponentially by repeating the verification, every time randomly choosing a challenge and its corresponding SLM2 setting from the database. The individual photon counts are added, and a combined threshold is set. As illustrated in Fig. 3d, after 10 repetitions

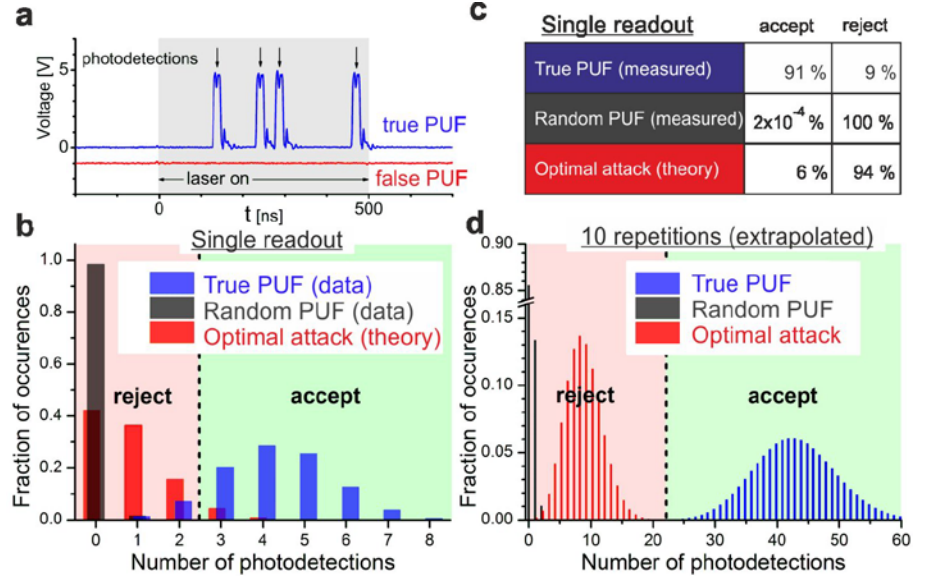


Figure 3| Quantum-secure readout of an unclonable physical key (PUF), using challenge pulses with 230 ± 40 photons distributed over 1100 ± 200 modes. **a**, Real-time examples for the true key (blue line) and a false key (red line, offset for clarity). **b**, Measured number of photodetections in case of the true key, a random key (imitated by sending random challenges to the same key), and for an optimal attack given $S=4$. The threshold is chosen such that the false positive and negative probabilities are approximately equally small assuming an optimal attack. **c**, Acceptance and rejection probabilities in case of the true key, a random key and in case of an optimal challenge-estimation attack. **d**, Number of photodetections extrapolated to 10 repetitions: the false positive and false negative probabilities quickly decrease to order 0.01 %.

the false accept and false reject probabilities are of order 10^{-4} . As detailed in the Appendix, after 20 repetitions they are both of order 10^{-9} . Thus, any desired level of statistical security can be reached in a small number of repetitions.

The time needed for readout is in practice limited by the switching time of the SLM, on the order of 100 ms for our SLM. However, using micromirror-based spatial light modulators that switch in $< 20 \mu\text{s}$ [27, 28], the complete authentication protocol with 20 repetitions can be performed in less than a millisecond. The one-time enrolment of the PUF then takes on the order of a second. Quantum-secure authentication does not require any secret information and is therefore invulnerable to adversaries characterizing the properties of the key (“skimming”). Hence, QSA provides a practical way of realizing unprecedentedly secure authentication of IDs, credit cards and even biometric keys [29].

Appendix

Shaping the challenge and response wavefronts

Two halves (referred to as SLM1 and SLM2) of the same reflective Holoeye HEO 1080P phase-only spatial light modulator are used to shape challenge wavefronts and decode response wavefronts, respectively. We use 50×50

segments, each consisting of 16x16 pixels, to shape challenge wavefronts. Since the used beams are cylindrical, the corners of the 50x50 segments area are not illuminated, so that we effectively use $2500\pi/4 = 1963$ segments of SLM1. Each segment is set to a phase of either 0 or π , allowing a total of $2^{1963} = 10^{591}$ different challenges, of which 1963 are orthogonal. This number is slightly larger than the number of modes that is supported by the sample area that we illuminate, which is experimentally verified to be 1100 ± 200 . The challenge is focused onto the PUF using a 0.95 NA 63x Zeiss microscope objective. The response is collected using the same objective and measured in 130x130 segments using standard phase-shifting interferometry [30]. This data is used to find the phases of the response wavefront at the 130x130 corresponding segments with in total 800x800 pixels on SLM2. SLM2 is then set to flatten the phase of the response wavefront by adding the conjugate phase to the response wavefront.

Security analysis

An adversary who does not have the PUF may attempt several attack strategies. We will address them here and show why they fail.

1) **Blinding attacks.** An additional detector which measures the total intensity outside the pinhole is sufficient to prevent false positive detections in case an adversary floods the system with light. In addition, flooding can be detected by including fake challenges, for which no photon detections are expected. The time needed for one repetition of the procedure is in practice limited only by the switching time of the SLM, on the order of 100 ms for the present SLM. Therefore there is ample room to randomly include fake challenges where (unknown to the adversary) no signal is expected. This also provides security against attacks that trigger the photodetector by non-optical means such as a beam of ionizing radiation.

2) A “**Challenge Estimation Attack**”, in which the adversary attempts to measure the challenge and then estimates the response. As shown in [25] for single photon states and in [31] for quadrature measurements, this is doomed to fail. A newer result [31] shows that when a challenge consists of $n < \sqrt{K}$ quanta in the same state, our scheme is secure against *all* challenge-estimation attacks. A quantitative example shows what the adversary can hope to achieve:

In our experiment the lower bound for the quantum security parameter S is 4. Assuming that the adversary has a perfect photon-counting or quadrature measuring camera, the expected squared inner product between the adversary’s best estimate and the correct challenge is equal to $1/(S+1) = 1/5$ [25]. He can therefore expect to obtain a number of photon clicks at the detector that is 1/5 times the expected number of clicks with the correct challenge. The expected

number of photons for the correct challenge is 4.3, so the attacker will obtain on average 0.8 photon clicks, well below the acceptance threshold of 3.

Experimentally we tested the scaling at the basis of this argument. We parameterize the challenge wavefronts by a K -dimensional complex vector C_0 . This C_0 is chosen by the verifier to yield the maximum light power in the focus behind SLM2 given the presence of the true PUF and the setting of SLM2. Now assume C_0 is replaced by another wavefront C_1 . We quantify the proximity of the challenge C_1 to the original challenge C_0 by the inner product $C_0 \cdot C_1 = \sum_{i=1..K} C_{0,i}^* \cdot C_{1,i}$, where the sum runs over the mode index. The fraction $|\gamma|^2$ of the light energy in the focus was experimentally found to scale as

$$|\gamma|^2 = 0.6 |C_0 \cdot C_1|^2,$$

confirming the scaling explained in [25].

3) Making a **passive optical device** that emulates the PUF functionality.

Since the PUF only realizes a complex linear transformation, one would be tempted to think that it is straightforward to make a passive optical device which does the same optical transformation as the PUF. It is not. The crucial point is that the adversary cannot know which challenge to expect, and therefore can only succeed if his passive optical device produces the correct response *for a large fraction of the possible* challenges. In other words, he will have to emulate a large fraction of the optical properties of the PUF into his optical device. This comes close to making a copy of the PUF. A *three-dimensional* random scattering medium with front surface area A contains much more random information than can be encoded in a random scattering surface of the same area A . For our sample parameters, a single diffraction-limited spot focused on the surface of the PUF gives rise to a speckle pattern with a Gaussian envelope with a Full Width at Half Maximum (FWHM) of approximately 5 μm , containing about 10^2 speckles. When we illuminate the PUF with a random challenge, the illumination spot is much larger than a diffraction-limited spot. The PUF is now seen to reflect a speckle pattern with a FWHM of about 15 μm , containing the equivalent of about 10^3 speckles. The reflection matrix describing the PUF is nonlocal (i.e., non-diagonal in any representation) as it connects surface points that are spatially separated by up to 5 μm . It is therefore impossible to emulate the PUF with a single scattering surface (e.g., that of an SLM), which would have a local reflection matrix.

An intriguing form of attack would be to make a PUF-emulating hologram into which a large portion of the PUF’s reflection matrix is written. Because of the low index of refraction contrast of photorefractive materials, on the order

of 0.02 to 0.1 [32], such a hologram must be significantly larger than the true PUF to obtain sufficient reflectivity. Therefore, this form of attack can be easily foiled using a light source with a coherence length of the order of 30 μm , on the order of the average path length photons travel in the PUF. The average optical path in the hologram is much longer than the coherence length so that no speckle pattern will form.

Another intriguing form of attack would be by means of a PUF-emulating nanophotonic network. Since in principle every passive linear optical network can be emulated by a sufficiently complex network of, e.g., beam splitters [33], this is in theory possible. Work by, e.g., Miller *et al.* [34, 35] show the concepts needed to make such a network. However, an adversary who wants to emulate the PUF functionality needs to program a passive optical device with N modes and N^2 connecting elements while keeping all the involved path lengths equal to within the coherence length. If the adversary has only a fraction F of the required number of elements, N^2 , the best he can hope to achieve is $|\gamma|^2 = F + (F-1)/(S+1)$.

Despite the huge efforts already spent in making linear optical networks for linear optical quantum computing and quantum simulation, state of the art networks have at maximum on the order of 10 connected beam splitters [36] and losses of 0.2 dB per element for waveguide-based beam splitters [37]. Recently larger networks have been built [38], but they only work because of the high tolerance against phase errors possible in the functionality of the realized phased arrays, which does not apply for a PUF

emulator. Alternative photonic-crystal-based networks could be smaller [39], but the corresponding losses are even higher. Hence, the extension to 10^6 connected nodes with overall losses of less than 10dB, extreme phase sensitivity and simultaneously keeping the differential path lengths to within 30 micrometer is still far out of reach of technology. If possible at all in future, it would require 10^6 optical elements each with a loss of less than 0.01 dB and a tremendous effort to emulate a single PUF.

A note about the scaling: For an N -mode PUF, the adversary needs to make a passive optical device with N^2 connecting elements. In our demonstration we have used on the order of 10^3 modes, but increasing this to 10^5 seems entirely feasible with present technology, given the availability of megapixel SLMs. With the state-of-the-art beam splitters [37], the required network of in the order of 10^{10} optical elements would have a loss of 20000dB and cover an area of the order of 1 m^2 .

4) **Hybrid strategies** that mix (complex) passive element and measuring devices. In the proof of the security against challenge-estimation attacks [31] no assumptions are made about the basis in which the adversary measures the challenge. Even if the adversary can program an arbitrary linear transformation before the measurement, he cannot breach the QSA scheme by estimating the challenge. In fact it is always better for the adversary to use his linear transformation capabilities directly on the challenge state as in attack 3.

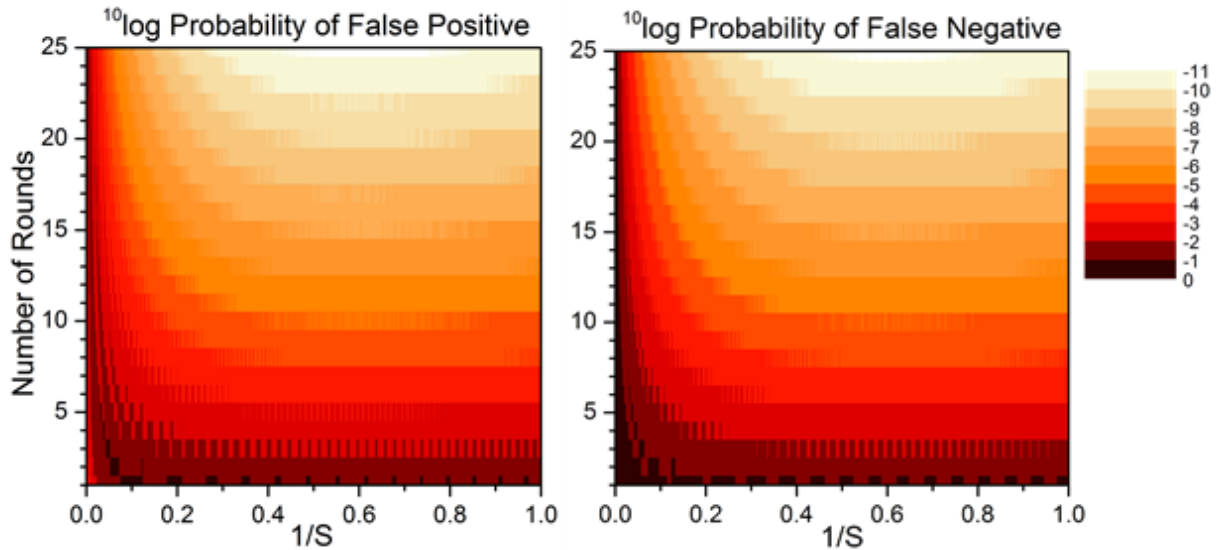


Figure A1| Probability of a false positive (acceptance of a challenge estimation attack) and a false negative decision (rejection of a correct PUF) as a function of the security parameter S and the number of repetitions (rounds). The plot is made by varying n and choosing the optimal threshold, while keeping $K = 1062$.

Repetition for exponential security gain

Fig. A1 shows the calculated probability of false-positive and false-negative decisions as a function of S and the number of repetitions, with the number of modes K kept constant. For each point in Fig. A1 the threshold was chosen in the minimum between the photon detection distributions obtained with the true PUF and the one calculated for the optimal challenge estimation attack. This leads to false positive and false negative probabilities that are approximately equally small. At a moderate S the probability of an erroneous decision is already of order 10^{-4} after 10 repetitions. At high S it takes more repetitions to rule out incorrect decisions since high S (at fixed K) implies a low photon number n . Since the threshold can only be taken at an integer number of photons, one may notice some quantization steps. For larger numbers of repetitions the probability of an incorrect decision is reduced exponentially and can hence be made arbitrarily small.

Correspondence and requests for materials should be addressed to P.W.H.P. (P.W.H.Pinkse@utwente.nl).

Acknowledgements We thank J. Bertolotti, K.-J. Boller, G. Giedke, J. Herek, S.R. Huisman, T.J. Huisman, B. Jacobs, A. Lagendijk, W.L. Vos, and G. Rempe for support and discussions. This work is partly funded by the Stichting voor Fundamenteel Onderzoek der Materie and STW, which are financially supported by the Nederlandse Organisatie voor Wetenschappelijk Onderzoek. A.P.M. acknowledges financial support from the European Research Council (grant number 279248).

[1] Pappu, R., Recht, B., Taylor, J. & Gershenfeld, N. Physical one-way functions. *Science* **297**, 2026 (2002).
 [2] Gassend, B., Clarke, D. E., van Dijk, M. & Devadas, S. Silicon physical unknown functions. In Atluri, V. (ed.) *ACM Conference on Computer and Communications Security — CCS 2002*, 148–160 (ACM, 2002).
 [3] Buchanan, J. D. R., Cowburn, R. P., Jausovec, A., Petit, D., Seem, P., Xiong, G., Atkinson, D., Fenton, K., Allwood, D. A. & Bryan, M. T. Forgery: ‘fingerprinting’ documents and packaging. *Nature* **436**, 475 (2005).
 [4] Tuyls, P., Schrijen, G. J., Škorić, B., van Geloven, J., Verhaegh, R. & Wolters, R. Read-proof hardware from protective coatings. In Goubin, L. & Matsui, M. (eds.) *Cryptographic Hardware and Embedded Systems — CHES 2006*, vol. 4249 of *LNCS*, 369–383 (Springer-Verlag, 2006).
 [5] DeJean, G. & Kirovski, D. Radio frequency certificates of authenticity. In *IEEE Antenna and Propagation Symposium — URSI (2006)*.
 [6] Tuyls, P., Škorić, B. & Kevenaar, T. (eds.) *Security with Noisy Data: Private Biometrics, Secure Key Storage and Anti-Counterfeiting* (Springer, London, 2007).
 [7] Guajardo, J., Kumar, S. S., Schrijen, G. J. & Tuyls, P. FPGA intrinsic PUFs and their use for IP protection. In Paillier, P. & Verbaudhede, I. (eds.) *CHES*, vol. 4727 of *LNCS*, 63–80 (Springer, 2007).
 [8] Sadeghi, A.-R. & Naccache, D. (eds.) *Towards Hardware-Intrinsic Security* (Springer, 2010).

[9] Bennett, C. H., Brassard, G., Breidbard, S. & Wiesner, S. Quantum cryptography, or unforgeable subway tokens. In *Advances in Cryptology: Proceedings of CRYPTO '82*, 267–275 (Plenum, 1982).
 [10] Bennett, C. H. & Brassard, G. Quantum cryptography: Public key distribution and coin tossing. *IEEE International Conference on Computers, Systems and Signal Processing* 175–179 (1984).
 [11] Bouwmeester, D., Ekert, A. & Zeilinger, A. *The Physics of Quantum Information* (Springer, 2000).
 [12] Nielsen, M. A. & Chuang, I. L. *Quantum Computation and Quantum Information: 10th Anniversary Edition* (Cambridge, 2010).
 [13] Mosk, A. P., Lagendijk, A., Leroose, G. & Fink, M. Controlling waves in space and time for imaging and focusing in complex media. *Nat. Photon.* **6**, 283 (2012).
 [14] Škorić, B., Tuyls, P. & Opey, W. Robust key extraction from physical uncloneable functions. In *Applied Cryptography and Network Security (ACNS)*, vol. 3531 of *LNCS*, 407 – 422 (Springer, 2005).
 [15] Tuyls, P., Škorić, B., Stallinga, S., Akkermans, A. H. M. & Opey, W. Information-theoretic security analysis of physical uncloneable functions. In Patrick, A. S. & Yung, M. (eds.) *9th Conf. on Financial Cryptography and Data Security*, vol. 3570 of *LNCS*, 141–155 (Springer, 2005).
 [16] Škorić, B. Quantum Readout of Physical Unclonable Functions. *Int. J. Quant. Inf.* **10**, 1250001–1 – 125001–31 (2012).
 [17] Wootters, W. K. & Zurek, W. H. A single quantum cannot be cloned. *Nature* **299**, 802 – 803 (1982).
 [18] Pinkse, P. W. H., Fischer, T., Maunz, P. & Rempe, G. Trapping an atom with single photons. *Nature* **404**, 365–368 (2000).
 [19] Peruzzo, A., Lobino, M., Matthews, J. C. F., Matsuda, N., Politi, A., Poullos, K., Zhou, X.-Q., Lahini, Y., Ismail, N., Wörhoff, K., Bromberg, Y., Silberberg, Y., Thompson, M. G. & O’Brien, J. L. Quantum walks of correlated photons. *Science* **329**, 1500–1503 (2010).
 [20] Wu, L.-A., Kimble, H. J., Hall, J. L. & Wu, H. Generation of squeezed states by parametric down conversion. *Phys. Rev. Lett.* **57**, 2520–2523 (1986).
 [21] Walbor, S. P., Lemelle, D. S., Almeida, M. P. & Ribeiro, P. H. S. Quantum key distribution with higher-order alphabets using spatially encoded qudits. *Phys. Rev. Lett.* **96**, 090501 (2006).
 [22] Salakhutdinov, V. D., Eliel, E. R. & Löffler, W. Full-field quantum correlations of spatially entangled photons. *Phys. Rev. Lett.* **108**, 173604 (2012).
 [23] S. Etcheverry and G. Cañas and E. S. Gómez and W. A. T. Nogueira and C. Saavedra and G. B. Xavier and G. Lima. Quantum key distribution session with 16-dimensional photonic states. *Sci. Rep.* **3**, 2316 (2013).
 [24] de Boer, J. F., van Rossum, M. C. W., van Albada, M. P., Nieuwenhuizen, T. M. & Lagendijk, A. Probability distribution of multiple scattered light measured in total transmission. *Phys. Rev. Lett.* **73**, 2567–2570 (1994).
 [25] Škorić, B., Mosk, A. P. & Pinkse, P. W. H. Security of quantum-readout PUFs against quadrature-based challenge-estimation attacks. *Int. J. Quant. Inf.* **11**, 1350041–1 – 1350041–15 (2013).
 [26] DiVincenzo, D. P. Towards control of large-scale quantum computing. *Science* **334**, 50 (2011).

- [27] Akbulut, D., Huisman, T. J., van Putten, E. G., Vos, W. L. & Mosk, A. P. Focusing light through random photonic media by binary amplitude modulation. *Opt. Express* **19**, 4017–4029 (2011).
- [28] Conkey, D. B., Caravaca-Aguirre, A. M. & Piestun, R. High-speed scattering medium characterization with application to focusing light through turbid media. *Opt. Express* **20**, 1733–1740 (2012).
- [29] Vellekoop, I. M. & Mosk, A. P. Focusing coherent light through opaque strongly scattering media. *Opt. Lett.* **32**, 2309 (2007).
- [30] Yamaguchi, I. & Zhang, T. Phase-shifting digital holography. *Opt. Lett.* **22**, 1268–1270 (1997).
- [31] Škorić, B. Security analysis of quantum-readout puffs in the case of generic challenge-estimation attacks. Submitted, <http://eprint.iacr.org/2013/479> (2013).
- [32] Barden, S. C., Arns, J. A. & Colburn, W. S. Volume-phase holographic gratings and their potential for astronomical applications. *Proc. SPIE* **3355**, 866 (1998).
- [33] Reck, M., Zeilinger, A., Bernstein, H. & Bertani, P. Experimental realization of any discrete unitary operator. *Phys. Rev. Lett.* **73**, 58–61 (1994).
- [34] Miller, D. A. B. All linear optical devices are mode converters. *Opt. Expr.* **20**, 23985 (2012).
- [35] Miller, D. A. B. Self-configuring universal linear optical component. *Phot. Research* **1**, 1–15 (2013).
- [36] Shadbolt, P. J., Verde, M. R., Peruzzo, A., Politi, A., Laing, A., Lobino, M., Matthews, J. C. F., Thompson, M. G. & O’Brien, J. L. Generating, manipulating and measuring entanglement and mixture with a reconfigurable photonic circuit. *Nat. Phot.* **6**, 45–49 (2011).
- [37] John, D. D., Heck, M. J. R., Bauters, J. F., Moreira, R., Barton, J. S., Bowers, J. E. & Blumenthal, D. J. Multilayer platform for ultra-low-loss waveguide applications. *IEEE Photon. Technol. Lett.* **24**, 876–878 (2012).
- [38] Sun, J., Timurdogan, E., Yaacobi, A., Hosseini, E. S. & Watts, M. R. Large-scale nanophotonic phased array. *Nature* **493**, 195–199 (2013).
- [39] Jiao, Y., Fan, S. & Miller, D. A. B. Demonstration of systematic photonic crystal device design and optimization by low-rank adjustments: an extremely compact mode separator. *Opt. Lett.* **30**, 141–143 (2005).